Ultrasonics Sonochemistry 38 (2017) 75–83

Contents lists available at ScienceDirect

Ultrasonics Sonochemistry

journal homepage: www.elsevier.com/locate/ultson

Stability of cavitation structures in a thin liquid layer

Wu Pengfei [a,b], Bai Lixin [a,*], Lin Weijun [a], Yan Jiuchun [c]

[a] State Key Laboratory of Acoustics, Institute of Acoustics, Chinese Academy of Sciences, Beijing 100190, China
[b] University of Chinese Academy of Sciences, Beijing 100049, China
[c] State Key Laboratory of Advanced Welding Production Technology, Harbin Institute of Technology, Harbin 150001, China

ARTICLE INFO

Article history:
Received 19 January 2017
Received in revised form 3 March 2017
Accepted 3 March 2017
Available online 6 March 2017

Keywords:
Ultrasonic cavitation structure
Stability
Cavitation bubble cloud
Perturbation

ABSTRACT

The inception and evolution of acoustic cavitation structures in thin liquid layers under different conditions and perturbations are investigated experimentally with high speed photography. The stability and characterization of cavitation structures are quantified by image analysis methods. It is found that cavitation structures (shape of bubble cloud and number of bubbles) are stable under unaltered experimental conditions, and the cavitation bubble cloud will return to the original structure and remain stable even in the face of large perturbations. When the experimental conditions are altered (for example, acoustic intensity, cavitation nuclei, boundary), the cavitation structures will vary correspondingly. Further analysis implies that the stability of cavitation structures is closely related to the number of bubbles in the cavitation bubble cloud. There are two mechanisms acting simultaneously in the cavitation bubble cloud evolution, one "bubble production" and the other "bubble disappearance". We propose that the two mechanisms acting together constitute the most likely explanation for the stability of cavitation structures and their transformation.

1. Introduction

Applications of ultrasonic cavitation span many industrial sectors, from sonochemistry, through ultrasonic cleaning, ultrasonic lithotripsy, sonoporation, emulsification, sludge reduction, nanoparticle preparation and wastewater treatment, to ultrasonic cell disruption [1,2]. It is generally known that cavitation bubble distribution is spatially inhomogeneous [3]. Numerous radially oscillating bubbles move translationally in the acoustic field. They are recognized with regularity to form different kinds of cavitation structures. For example, conical bubble structure (CBS) [4–6], acoustic Lichtenberg figure (ALF) [7–9], tailing bubble structure (TBS) [10,11], jet-induced bubble structure (JSB) [10,11], smoker structure [12]. It was found that the specific filament branches in ALF structures possess a remarkable high stability and long lifetime [3]. Ulrich Parlitz [8] (1999) and Robert Mettin [13] (1999) reproduced ALF structures in simulations by the assumption of an inhomogeneous distribution of bubble sources in space. Based on the theory of shape instability and diffusive instability for single bubbles, Zhang Wenjuan [14] (2013) studied the instability of an individual bubble in a bubble chain (a filament branch in ALF structures). Alexei Moussatov [4,15] (2003) found that the macro-structure of the CBS in the vicinity of the radiating surface remains remarkably stable, though the streamers in the structure are not stable and fluctuate in space. Bertrand Dubus [5] (2010) and Olivier Louisnard [6] (2012) proposed some explanations for the physical origin of the CBS from different angles. Bai Lixin [12] (2012) found that smoker structures are not stable in long rang and it is hard to predict their positions, however their shape and internal structures are rather stable. He also investigated the control of TBS and JBS by artificial implants of nuclei based on their stability [10,11].

Although similar phenomena of cavitation-structure stability have been observed by many others, detailed experimental study on the macro stability can be rarely find. The details of cavitation structure are usually difficult to be observed and unsuitable for stability studies because of its three dimensional shape and complex mass transfer process with surroundings. To overcome the difficulty, the cavitation structures in thin liquid layers (between two parallel solid walls) are used to investigate the stability of cavitation structures, because the quasi-2D structure can be clearly photographed and easily controlled. The cavitation in thin liquid layer was first investigated by Alexei Moussatov [16] (2005). He found that this configuration lead to a large amplification of the acoustic pressure which makes the generation of cavitation possible at low power or in a wide frequency range. García-Atance Fatjó [17] (2010) investigated the cavitation ring in a thin liquid layer using

* Corresponding author.
E-mail address: blx@mail.ioa.ac.cn (L. Bai).

http://dx.doi.org/10.1016/j.ultsonch.2017.03.002
1350-4177/

a theoretical model based on the combination of Fluid Mechanics and Analytical Mechanics. We have already studied the memory effect [18] and surface tension [19] of cavitation structures in a thin liquid layer, and the stability of cavitation structures will be discussed in this paper.

2. Experiment

Fig. 1 illustrates the experimental setup when recording the cavitation structure in the thin liquid layer. The experimental setup in Fig. 1(A) consisted of the ultrasonic cavitation devices, the high-speed imaging and illumination system, step motor-driven gap adjusting system, etc (the experimental setup photo see also Bai et al. [10] (2014)). The piezoceramic sandwich transducer is well enveloped and can be submerged in water completely. The ultrasonic horn is mounted horizontally in a transparent chamber (600 mm × 330 mm × 330 mm). Fresh tap water (with many nuclei) is used in the experiment so as to reduce the cavitation threshold. The high power ultrasound is produced by two ultrasonic processors (Jiuzhou Ultrasonic Technology Co., Ltd. China) with a frequency of 18.5 kHz (radiating surface diameter: 50 mm) and 40 kHz (radiating surface diameter: 30 mm) and a maximum input electric power of 100 W. The radiating surface diameter of the sandwich piezoelectric ceramic ultrasonic transducer equals to the diameter of piezoelectric plate. Step motor-driven gap adjusting system (minimum adjustment distance: 20 μm) is used to fix the transducer and adjust the distance (liquid layer thickness) between the radiating surface and transparent reflection plane (glass plate thickness: 5 mm) in the experiment. Cavitation structure is recorded with a high-speed camera (Photron Fastcam SA-1, Photron Ltd., Japan) equipped with two long distance microscopes (Zoom 6000, Navitar, USA; LM50JCM, Kowa, Japan) respectively. The pictures are taken in a framing rate of 500 fps (1024 × 1024 pixels and 20 μm pixel size) to 54,000 fps (320 × 256 pixels) for the whole or the part of cavitation structures. The frames are illuminated with PI-LUMINOR high-light LED lamp (150 W) and HYLOW xenon flash lamp (duration time: 4 ms). The minimum size of observable bubbles in the experiment is about 2 μm.

In order to record the motion of cavitation bubbles in a large magnification, the experimental setup was rearranged (as shown in Fig. 1(B)). The ultrasonic horn is mounted perpendicularly in a cylindrical chamber (diameter: 12 cm). A frosted glass (thickness: 1 mm) is bonded to the radiating surface. The reflected light is scattered by a frosted glass to illuminate the bubbles. The positions of light source and mirror were adjusted for a better photographic effect.

3. Results and discussion

Fig. 2 shows the inception of cavitation structures, when h = 0.82 mm, where h is the thickness of liquid layer. Scatter light is used to illuminate the bubbles which are bright in the pictures. Acoustic intensity increases rapidly after turning on the ultrasonic transducer, and some free bubble nuclei expand to visible size (τ = 2 ms) under the influence of the sound field. Then, these tiny bubbles gradually grow up and split, forming bubble clusters (τ = 10 ms). These bubble clusters continue to spread and cross-link with each other (τ = 26 ms), which forms disc-shaped structures (τ = 509 ms–2069 ms). The characteristic of disc-shaped cavitation structures is their curved boundary. Non-cavitation regions (dark areas) form pore structure (as shown the subfigure (τ = 2069 ms) in Fig. 2). We have studied the mechanism on the formation of disc-shaped structures in Reference [19]. Although the distribution of cavitation regions and disc-shaped non-cavitation regions changes every now and then, the whole shape is similar (the structures consist of elements with disc-shaped features). The high speed photography data in 4 s (it is a long time compare to the evolution of cavitation bubble cloud) are analyzed, it is found that the number (5–7, see lower left Fig. 2) and the diameter (7 mm–20 mm, see lower right Fig. 2) of the disc-shaped structures keep relative stable. So the distribution of cavitation bubble cloud (τ = 839 ms–2069 ms) can be regarded as a quasi-steady cavitation structure. If the state (τ = 0 ms) was regarded as a cavitation structure, it is reasonable to consider that acoustic intensity is responsible for the inter-transformation between cavitation structures.

Fig. 3 shows the inception of cavitation structure, when h = 1.23 mm. The evolution is similar to Fig. 2, but the final distribution of bubble cloud is different, specifically rod-shaped quasi-steady cavitation structures (τ = 1312 ms–5062 ms). The characteristic of rod-shaped cavitation structures is their straight boundary. The cavitation clouds look like rods, and non-cavitation regions (dark areas) form polygon structure (as shown the subfigure (τ = 5062 ms) in Fig. 3). The mechanism of the formation of rod-shaped structures will be discussed in the future. It can be seen from Fig. 3 that the number (5–7, as shown the subfigure in the lower left corner of Fig. 3) and the length (7 mm-20 mm, as shown the subfigure in the lower right corner of Fig. 3) of rod-shaped structures keep relative stable. Comparing Fig. 2 with Fig. 3, it can be found that the thickness of liquid layer is different except that the initial acoustic intensity and other conditions are the same. As a consequence, the final cavitation structure is different.

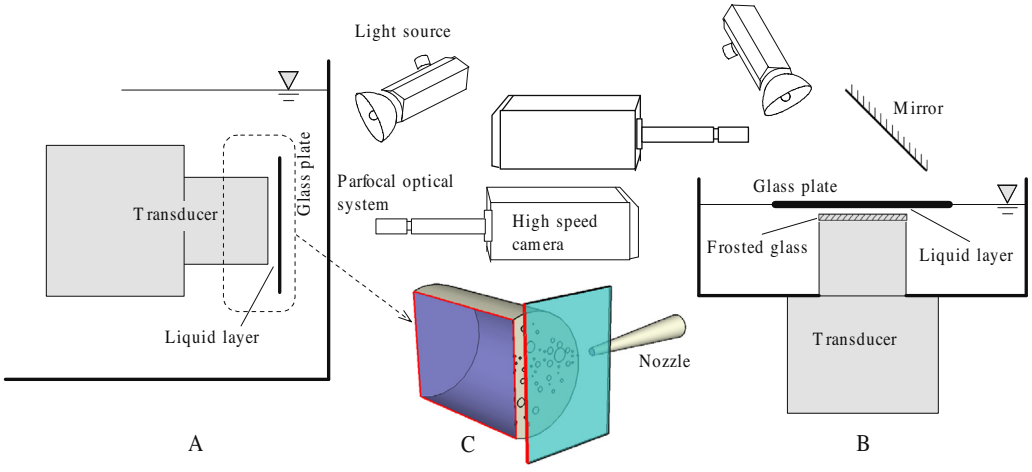

Fig. 1. Experimental setup.

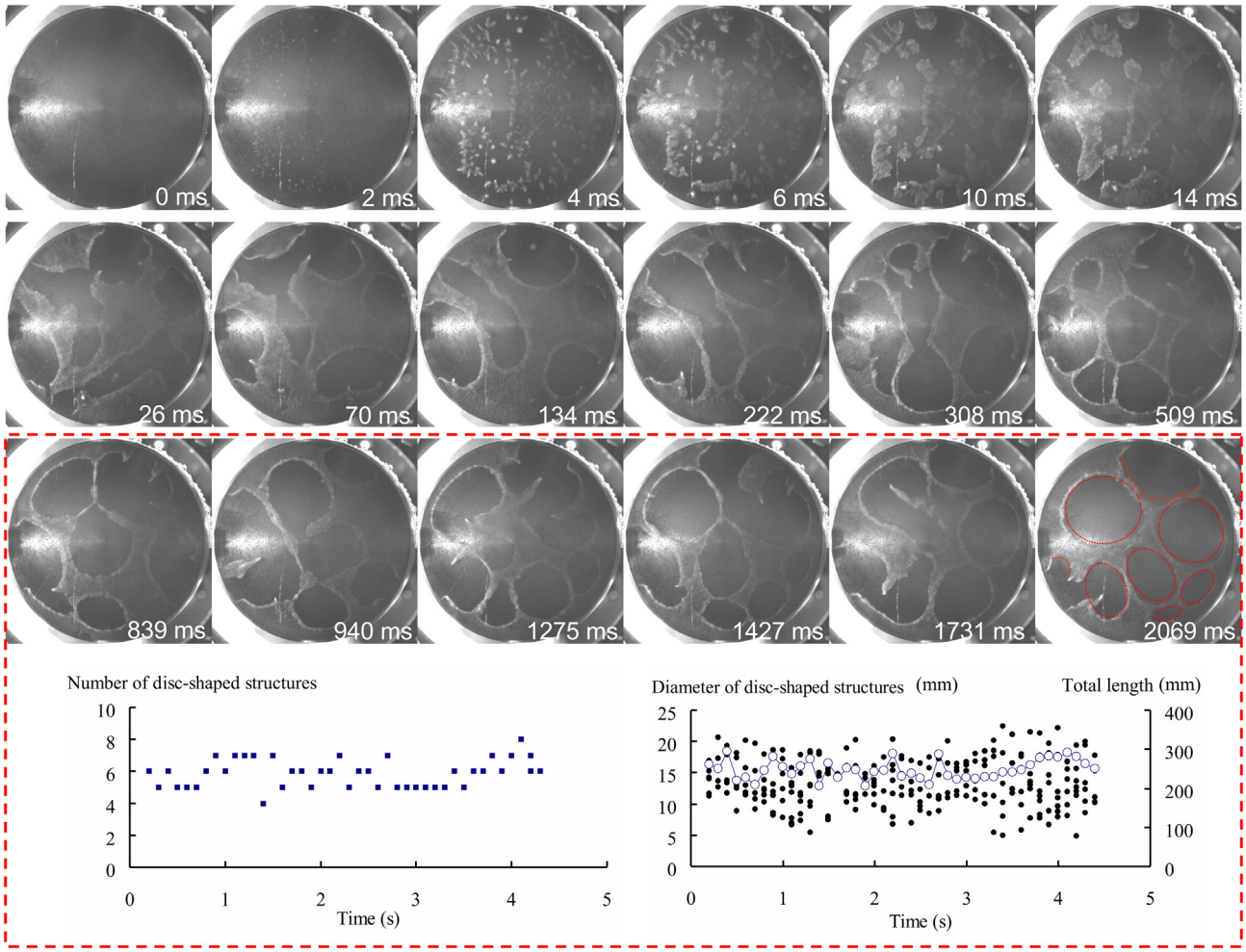

Fig. 2. Morphological stability of cavitation structures (disc-shaped) (f = 20 kHz, h = 0.82 mm).

Instead of studying the formation mechanism of individual disc-shaped cavitation structure [19], the focus of this paper is on the macro stability of the whole cavitation structures in thin liquid layers. Rod-shaped structures and disc-shaped structures are merely taken as the characterizations of stability of the whole cavitation structures in the thin liquid layers. Their formation mechanism plays a minor role in this study and is not the focus of this paper.

Except for acoustic intensity and boundary, the fluctuation of bubble nuclei can also cause the transformation of cavitation structures (as shown in Fig. 4). When a water jet which is produced by using a nozzle filled with water impacts on the cavitation structure (as shown in Fig. 1C, for a better presentation, a section plane figure is used to show the position of the nozzle), fresh bubble nuclei carried by the jet reduces cavitation threshold. Driven by ultrasound, a lot of nuclei develop into cavitation bubbles; then a bubble cloud comes into being [10] and gradually covers the whole interspace of the liquid layer. When the water jet moves away, the cavitation bubble cloud remains steady for 0.5 s, and then it shrinks and recovers to the quasi-steady disc-shaped structure (similar to the structure in Fig. 2). Similarly, the cavitation structure (as shown in Fig. 3) can also recover to its original quasi-steady state from the water jet perturbation (as shown in Fig. 5). Therefore, cavitation cloud can return to the initial structure and remain stable even in the face of great perturbations. Furthermore, if the liquid jet keeps steady, the cavitation structures (as shown the subfigure when τ = 194 ms in Fig. 4 and the subfigure when τ = 262 ms in Fig. 5) will remain stable.

Figs. 2 and 3 were photographed with low optical magnification and long exposure time, and the cavitation clouds seem to be almost continuous distributed. The bubbles in a cavitation cloud can be clearly distinguished with high optical magnification and short exposure time. Although a cavitation cloud is quite random in spatial and temporal scale of bubble oscillation, it shows statistical regularity in large spatial and long temporal scale. Fig. 6(A) shows the time snapshot when the layer thickness increases from nearly 0 mm to 2 mm at a constant speed with the controlling of a step motor-driven gap adjusting system, it is found that the diameter of cavitation bubble decreases with the decrease of the layer thickness, correspondingly, the diameter of cavitation bubble increases with the increase of the layer thickness (as shown in Fig. 6(B)). A large number of experiments show that the qualitative relationship is quite universal in the span of the layer thickness in present experiment. Fig. 7 shows the inception and disappearance process when layer thickness fix on 0.8 mm. it is found that the distribution density of the cavitation bubbles is inhomogeneous, smoker cavitation cloud, rod-shaped cavitation cloud and the boundary of the cavitation cloud have a higher distribution density (8–12 bubbles per square millimeter) than other region (5–8 bubbles per square millimeter). The distribution density of cavitation bubbles is relatively stable. Because the shape of the cavitation structures is quite stable, the total boundary length keep relative

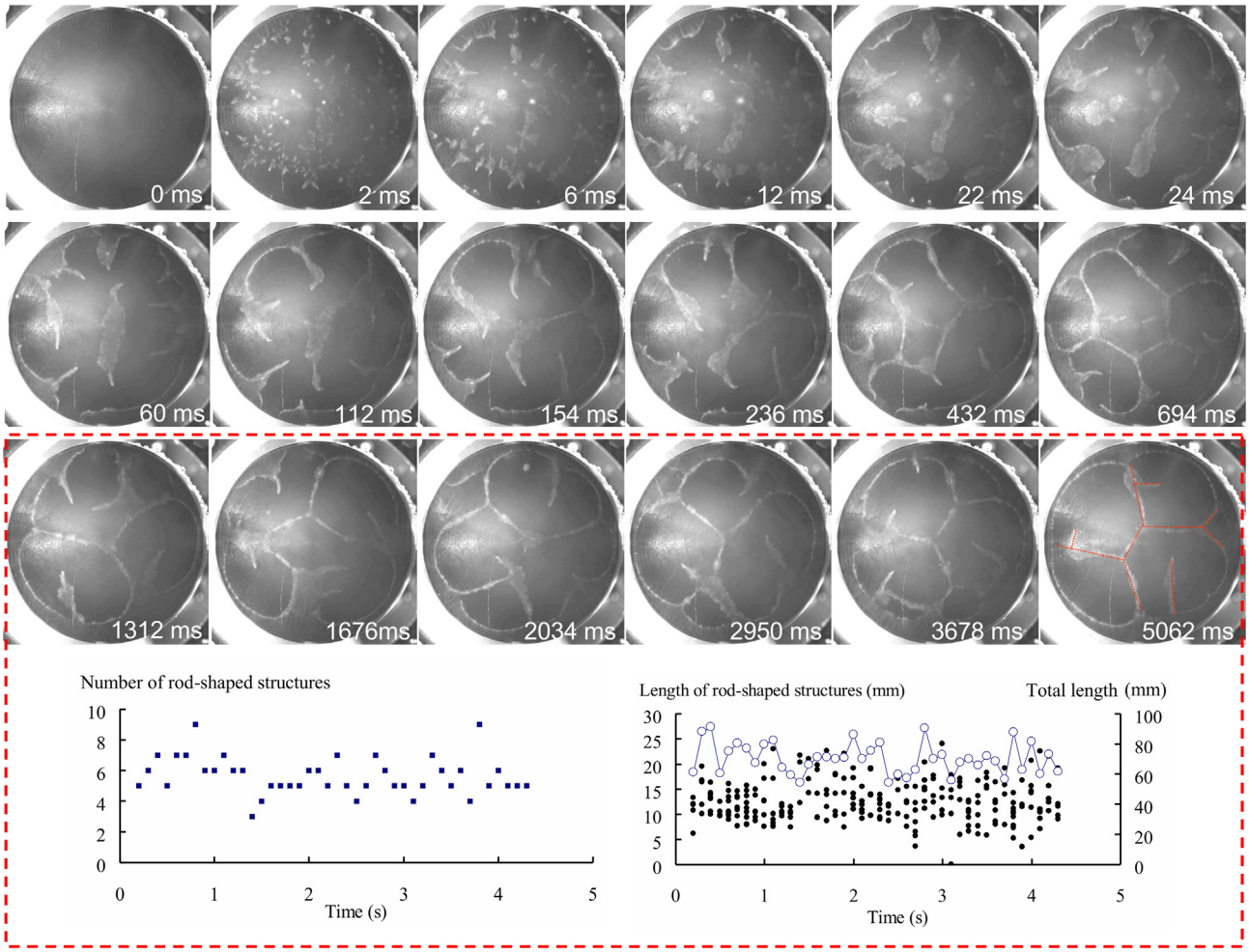

Fig. 3. Morphological stability of cavitation structures (rod-shaped) (f = 20 kHz, h = 1.23 mm).

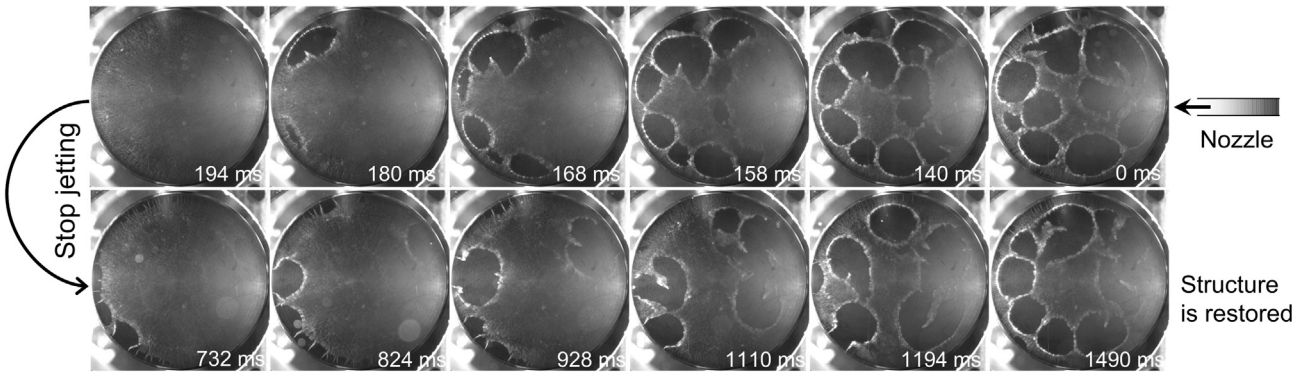

Fig. 4. Evolution of cavitation structure when a liquid jet impact from the right side (disc-shaped) (f = 20 kHz, h = 0.82 mm).

stable (see Figs. 2 and 3, the total length of rod-shaped structures keep relative stable, the total circumference of the disc-shaped structures keep relative stable). So the macro area of cavitation bubble cloud can be used to estimate the number of cavitation bubbles.

Fig. 8 shows the method to measure the area of cavitation cloud. A clearly boundary distinguishes the cloud region and water region, and scarcely any observable cavitation bubbles can be found in the liquid region (dark area). First, subtract the image (A) from (B) to remove the background. Then an image with black background and bright cavitation cloud is obtained (as shown in Fig. 8(C)). Finally, binarization is applied to the images (as shown in Fig. 8(D)).

The percentage area of cavitation cloud can be calculated by the pixel area of the white regions divided by the transducer radiation surface [20]. Nearly 10,000 images photographed with 500 fps in 4 experiments are all processed like this. Time evolution curves of cavitation area percentage can be obtained (as shown in Fig. 9). It can be seen that the percentage increases dramatically from 0 to near 40%, then keep relatively stable when h = 0.82 mm; the

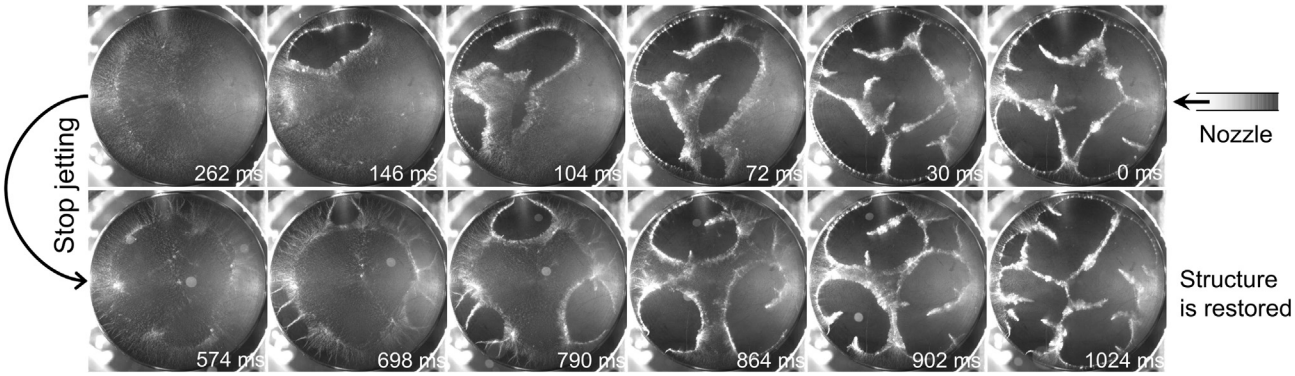

Fig. 5. Evolution of cavitation structure when a liquid jet impact from the right side (rod-shaped) (f = 20 kHz, h = 0.82 mm).

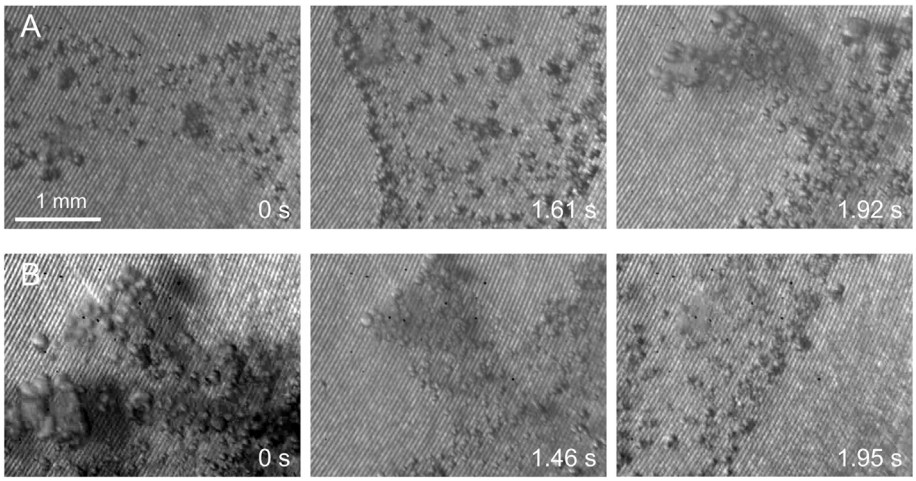

Fig. 6. Variation of bubble diameter with liquid layer thickness (f = 20 kHz).

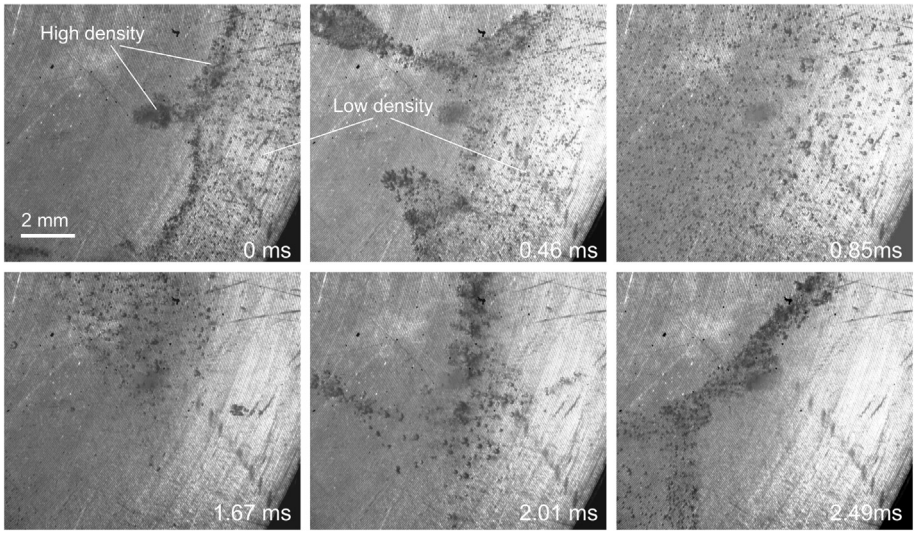

Fig. 7. Bubble density distribution in the cavitation structures (f = 20 kHz).

percentage jumps from 0 to near 26%, then keep relatively stable when h = 1.32 mm. Although cavitation bubble distribution in liquid layer keeps moving, the area of cavitation cloud (the number of cavitation bubbles) is fairly stable. So the similar distribution of cavitation bubble cloud in certain gap distance can be regarded as a quasi-steady cavitation structure. When the cavitation structure suffers from a perturbation of nuclei caused by water jet, the area percentage undergoes a fluctuation. When the liquid jet stops, the area percentage recovers to its original value. It can be seen that cavitation structures (shape of bubble cloud and number of bubbles) have stability against transient perturbation. It should be noted that the periodic bursts in the percentage for h = 0.82

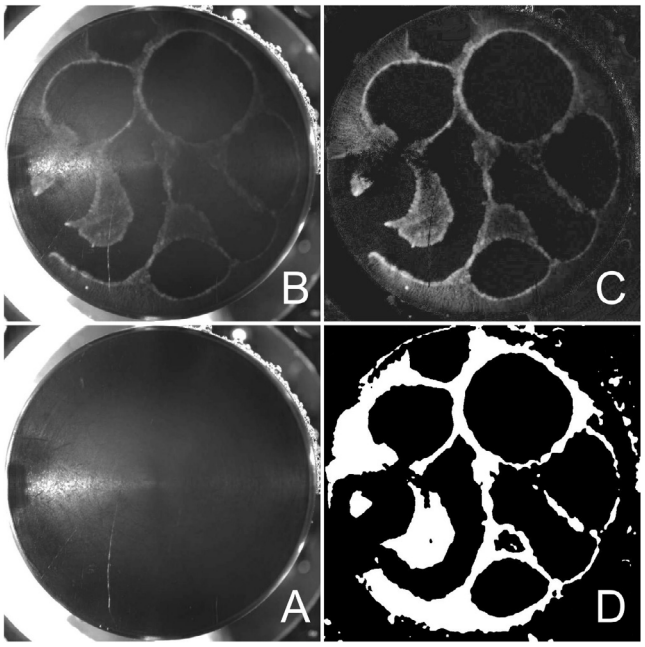

Fig. 8. Example of converting the grayscale images to binary images for the cavitation area. (A) Radiating surface before turning on the transducer. (B) Cavitation structure on the radiating surface after turning on the transducer. (C) Background removal. (D) Binarization.

(red line) and h = 1.23 (pink line), with a periodicity about 2 s. This is due to the "water jet" mentioned above; the "period" is just the interval between twice operations of jet impingement using a nozzle filled with water, because we operate the nozzle about once 2 s, so the "periodicity" does not have other physical meaning.

Fig. 10 shows the transformation of cavitation structures, it is photographed with a frame speed of 1000 fps. The liquid layer is controlled by a step motor-driven gap adjusting system. The layer thickness decreases at the same speed from 3 mm to nearly 0 mm and then increases from 0 mm to 4 mm. Images are analyzed as above. It is found that the area of cavitation bubble cloud increases with the decrease of layer thickness and vice versa, which means that cavitation structures (shape of bubble cloud and number of bubbles) transform to another steady state when boundary is altered and recover to original state when boundary is back to the original circumstance.

When a cavitation bubble cloud changes from one structure to another, the number of cavitation bubbles also changes. Fig. 11 shows the process of a gas bubble splitting to a cluster of cavitation bubbles when the transducer is just turned on. Fig. 12 shows the coalescence of cavitation bubbles when the transducer is just turned off. The special structure of thin liquid layer makes it doable to count the number of cavitation bubbles. The two examples illustrate the influence of acoustic intensity on the number of cavitation bubbles.

Fig. 13 shows the variation of bubble numbers in a cluster when acoustic intensity is nearly constant. The lens was focused on a bubble cluster, which is well-defined and numerable when the bubbles expand to their maximum volume. Some cavitation bubbles may split, merge or annihilate, some bubbles may be too small to be visible, and some bubbles may suddenly grow to visible size. All of these factors influence the number of cavitation bubbles in an acoustic period.

There are two opposite physical processes: bubble production and bubble disappearance, which may coexist in the cavitation bubble cloud. The rate of bubble production is defined as the increased number per unit of time relative to the original bubbles number. The increased number may be from fragmentation, suddenly growing up to sufficient size to be visible of cavitation bubbles or other possible way [21]. The rate of bubble disappearance is defined as the decreased number per unit of time relative to the original bubbles number. The decreased number may be from coalescence, annihilation, dormancy (It means that cavitation bubbles become too small to be visible and look like inactive, but they do not annihilate over several cycles and some of them may be active after a while.) or other possible way. If the rate of bubble production equals to the rate of bubble disappearance during a period of time, then the number of cavitation bubbles remains unchanged, and cavitation structure is steady or quasi-steady. Fig. 14A shows the transformation and stability mechanism of cavitation structures. The horizontal coordinate represents the acoustic power penetrating the cavitation cloud. The longitudinal coordinate represents the total number of cavitation bubbles in the cavitation cloud. When experimental conditions have a perturbation, the rate of bubble production and disappearance loses balance for a moment, and then recover balance under a negative feedback mechanism (as shown the arrows surrounding steady-state A in the Fig. 14A). "a" represents that the rate of bubble production is greater than the rate of bubble disappearance, the number of cavitation bubbles increases, the area of cavitation cloud increases; "b" represents that the acoustic power applied to the liquid decreases due to the shielding effect of cavitation cloud. "c" represents that the rate of bubble disappearance is greater than the rate of bubble production, the number of cavitation bubbles decreases due to the decrease of acoustic power applied to liquid. "d" represents that the acoustic power applied to the liquid increase due to the weakening of shielding effect. The whole process tends to self-stabilize the system and keep the state stable.

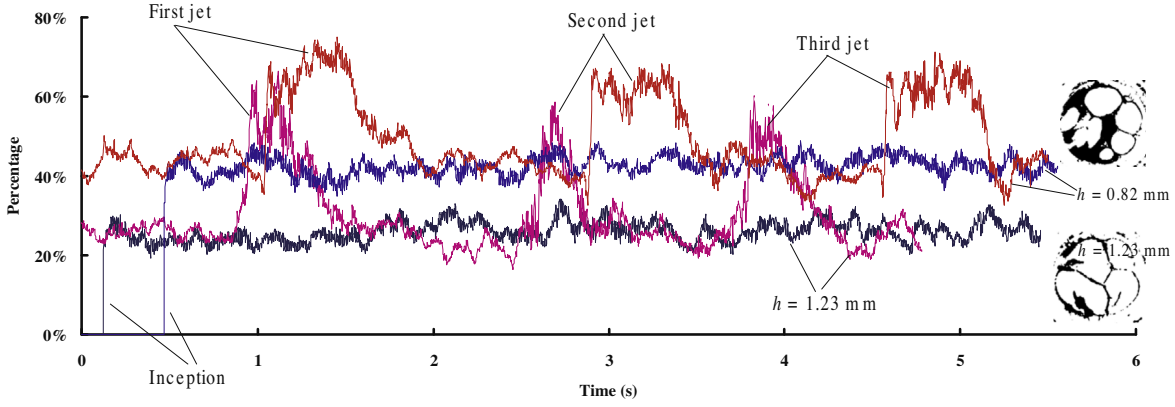

Fig. 9. Variation of cavitation area with time (f = 20 kHz).

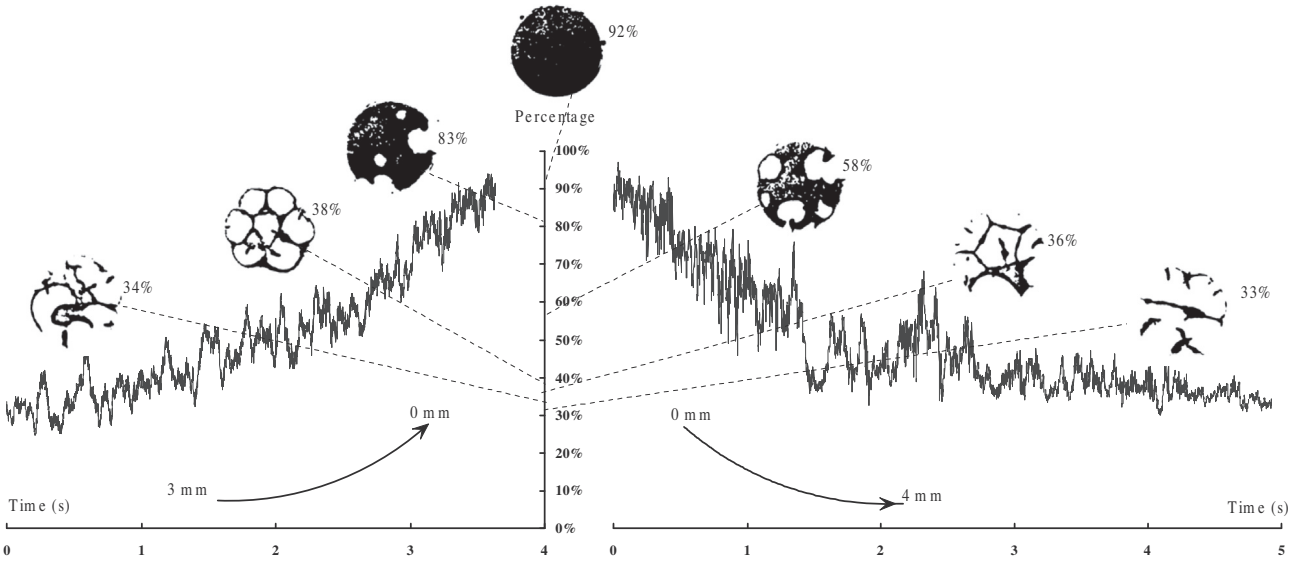

Fig. 10. Variation of cavitation area with liquid layer thickness and time (f = 40 kHz).

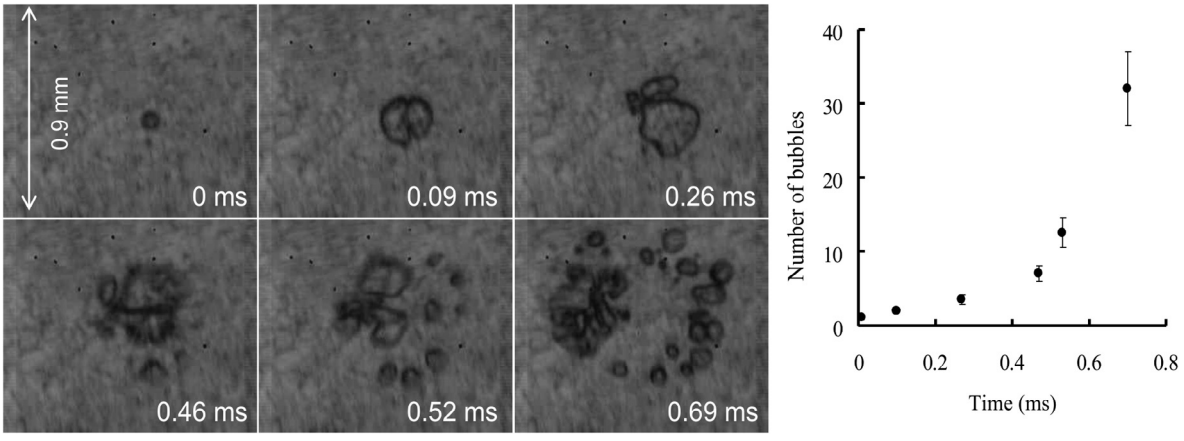

Fig. 11. Fragmentation of cavitation bubbles (f = 20 kHz).

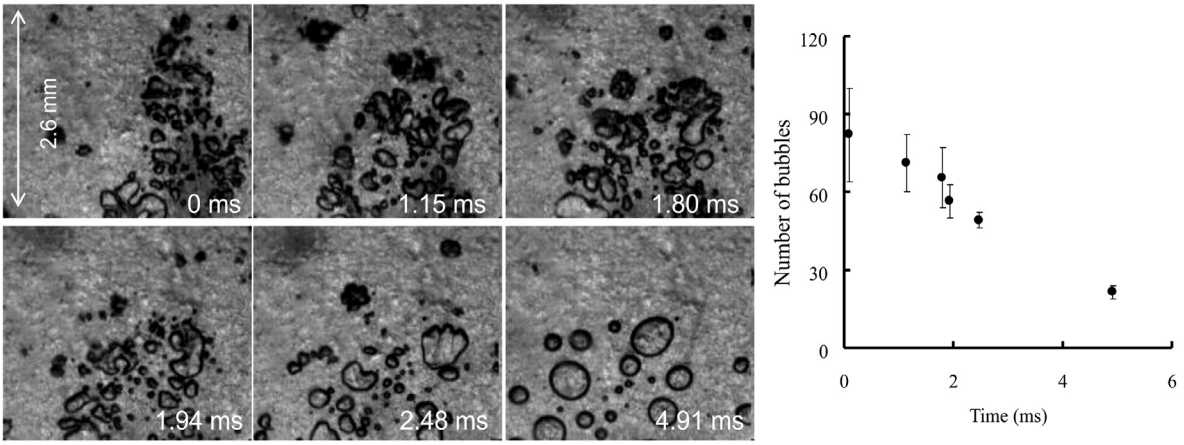

Fig. 12. Coalescence of cavitation bubbles (f = 20 kHz).

If the rate of bubble production is not equal to the rate of bubble disappearance, then the number of cavitation bubbles changes, cavitation bubble cloud may evolve into another kind of cavitation structure. The steady-state A, B, C and D in Fig. 14A are four steady states of cavitation structures under different conditions, the rate of bubble production and disappearance keeps balance, the total number of cavitation bubble remains unchanged. When the experimental conditions are altered, the rate of bubble production and

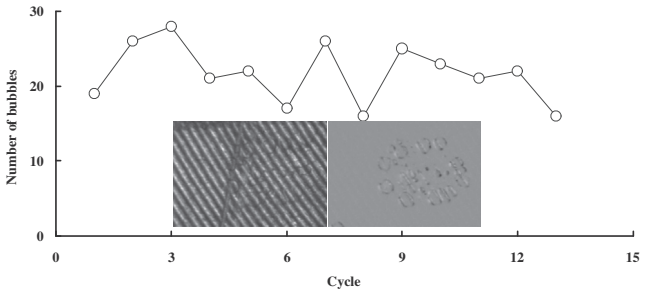

Fig. 13. Variation of bubble number for a cavitation cluster (f = 20 kHz).

disappearance loses balance, the cavitation structures vary correspondingly, and the variation is relative reversible. The increase and decrease of bubble production and disappearance rate is related to the changes of acoustic intensity, bubble nuclei and boundary. For example, steady-state A to steady-state B is the transformation caused by the decrease of acoustic intensity. The rate of bubble disappearance is greater than the rate of bubble production, cavitation bubble number decreases. Steady-state A to steady-state C is the transformation caused by the increase of nuclei. The rate of bubble production is greater than the rate of bubble disappearance, cavitation bubble number increases. However, the increase of cavitation bubble number enhances shielding effect of cavitation cloud; hence acoustic power applied to liquid weakens. Steady-state A to steady-state D is the transformation caused by the increase of liquid layer thickness (boundary). The rate of bubble disappearance is greater than the rate of bubble production, cavitation bubble number decreases. The acoustic power penetrating the cavitation cloud increases [19]. This is because that the boundary effect is weakened when liquid layer thickness increases, which facilitates the migration and coalescence of cavitation bubbles under the action of second Bjerknes force.

Fig. 14B shows that the structures are quite stable, cavitation structures in thin liquid layers have stability against transient perturbation to keep and recover to its original shape and bubble numbers. When the experimental conditions change (for example, acoustic intensity, cavitation nuclei, boundary), the cavitation structures will vary correspondingly and then remain stable over time.

4. Summary and conclusions

The distribution of cavitation bubbles is spatially inhomogeneous; they can form different structures in the ultrasound field. Although the motion of individual bubbles in cavitation structures is quite disordered and unpredictable, our experiments also find that the structures are quite stable, cavitation structures in thin liquid layers have stability against transient perturbation to keep and recover to its original shape and bubble numbers. When the experimental conditions change (for example, acoustic intensity, cavitation nuclei, boundary), the cavitation structures will vary correspondingly and then remain stable over time. There exist two processes acting simultaneously in the cavitation bubble cloud evolution, one "bubble production" and the other "bubble disappearance". A competition and dynamic balance of the two processes with a negative feedback mechanism has been proposed to explain the stability of cavitation structures and their transformation.

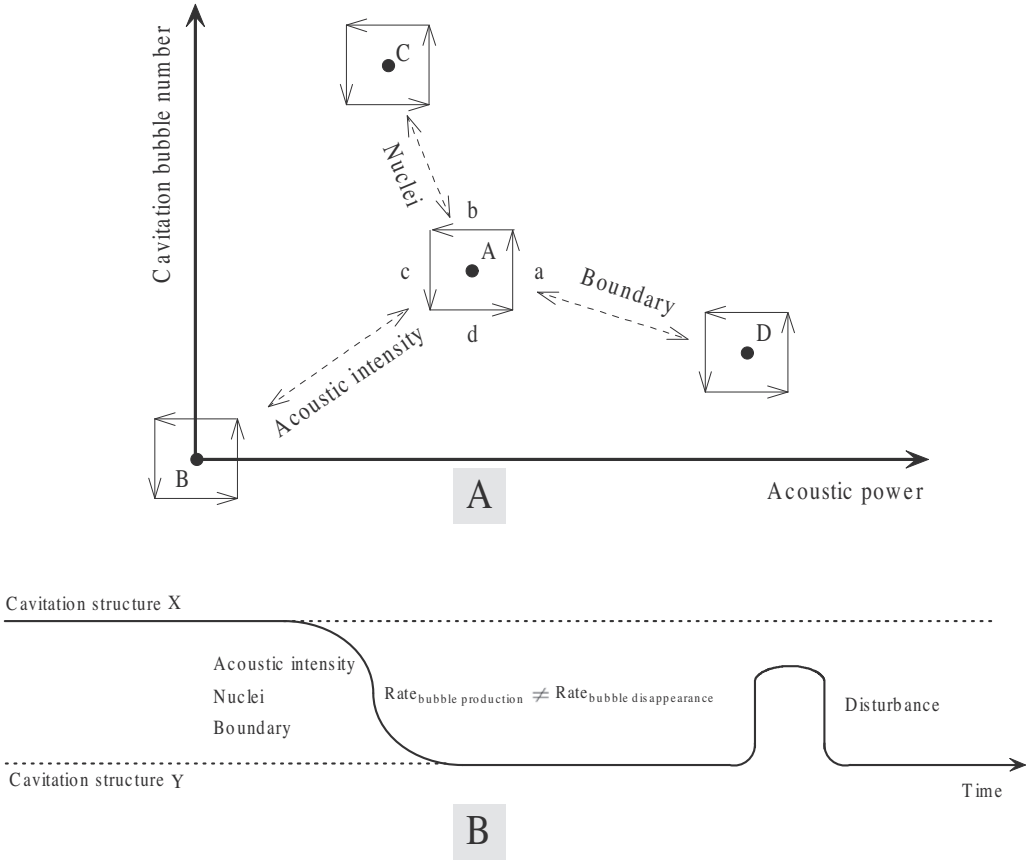

Fig. 14. Schematic diagram of transformation and stabilization of cavitation structures. A, B, C, D, X and Y represent steady states of cavitation structures; a,b,c and d represent four processes which form a closed loop negative feedback.

Acknowledgments

The authors would like to thank Mr. Xiuming Wang for inspiring the present work. This work was supported by the National Natural Science Foundation of China (No. 11674350) (No. 11174315) (No. 51435004).

References

[1] L. Bai, W. Xu, Z. Tian, N. Li, A high-speed photographic study of ultrasonic cavitation near rigid boundary, J. Hydrodyn. 20 (2008) 637–644.
[2] Juan A. Gallego-Juárez, Karl F. Graff (Eds.), Power Ultrasonics: Applications of High-Intensity Ultrasound, Elsevier, 2014.
[3] R. Mettin, Bubble structures in acoustic cavitation, in: A.A. Doinikov (Ed.), Bubble and Particle Dynamics in Acoustic Fields: Modern Trends and Applications, Research Signpost, Kerala, 2005, pp. 1–36.
[4] A. Moussatov, C. Granger, B. Dubus, Cone-like bubble formation in ultrasonic cavitation field, Ultrason. Sonochem. 10 (2003) 191–195.
[5] B. Dubus, C. Vanhille, C. Campos-Pozuelo, C. Granger, On the physical origin of conical bubble structure under an ultrasonic horn, Ultrason. Sonochem. 17 (2010) 810–818.
[6] O. Louisnard, A simple model of ultrasound propagation in a cavitating liquid. Part II: Primary Bjerknes force and bubble structures, Ultrason. Sonochem. 19 (2012) 66–76.
[7] I. Akhatov, U. Parlitz, W. Lauterborn, Towards a theory of self-organization phenomena in bubble–liquid mixtures, Phys. Rev. E 54 (1996) 4990–5003.
[8] U. Parlitz, R. Mettin, S. Luther, I. Akhativ, M. Voss, W. Lauterborn, Spatio-temporal dynamics of acoustic cavitation bubble clouds, Philos. Trans. R. Soc. Lond. A 357 (1999) 313–334.
[9] R. Mettin, S. Luther, C.-D. Ohl, W. Lauterborn, Acoustic cavitation structures and simulations by a particle model, Ultrason. Sonochem. 6 (1999) 25–29.
[10] L. Bai, J. Deng, C. Li, D. Xu, W. Xu, Acoustic cavitation structures produced by artificial implants of nuclei, Ultrason. Sonochem. 21 (2014) 121–128.
[11] L. Bai, W. Xu, J. Deng, C. Li, D. Xu, Y. Gao, Generation and control of acoustic cavitation structure, Ultrason. Sonochem. 21 (2014) 1696–1706.
[12] L. Bai, C. Ying, C. Li, J. Deng, The structures and evolution of Smoker in an ultrasonic field, Ultrason. Sonochem. 19 (2012) 762–766.
[13] R. Mettin, S. Luther, C.D. Ohl, W. Lauterborn, Acoustic cavitation structures and simulations by a particle model, Ultrason. Sonochem. 6 (1999) 25–29.
[14] W. Zhang, Y. An, Instability of a bubble chain, Phys. Rev. E 87 (2013) 1558–1561.
[15] A. Moussatov, R. Mettin, C. Granger, T. Tervo, B. Dubus, W. Lauterborn, Evolution of acoustic cavitation structures near larger emitting surface, in: Proceedings of the WCU, Paris, France, 2003, pp. 955–958.
[16] A. Moussatov, C. Granger, B. Dubus, Ultrasonic cavitation in thin liquid layers, Ultrason. Sonochem. 12 (2005) 415–422.
[17] G.G.-A. Fatjó, A.T. Pérez, M. Hadfield, Experimental study and analytical model of the cavitation ring region with small diameter ultrasonic horn, Ultrason. Sonochem. 18 (2011) 73–79.
[18] L. Bai, W. Lin, P. Wu, J. Deng, C. Li, D. Xu, D. Wang, L. Chen, Memory effect and redistribution of cavitation nuclei in a thin liquid layer, Ultrason. Sonochem. 32 (2016) 213–217.
[19] L. Bai, X. Chen, G. Zhu, W. Xu, W. Lin, P. Wu, C. Li, D. Xu, J. Yan, Surface tension and quasi-emulsion of cavitation bubble cloud, Ultrason. Sonochem. 35 (2017) 405–414.
[20] T. Wang, Z. Xu, T.L. Hall, J.B. Fowlkes, C.A. Cain, An efficient treatment strategy for histotripsy by removing cavitation memory, Ultrasound Med. & Biol. 38 (2012) 753–766.
[21] L. Bai, W. Xu, C. Li, Y. Gao, The counter jet formation in an air bubble induced by the impact of shock waves, J. Hydrodyn. 23 (2011) 562–569.